

## Solution Processed High-Performance of p-Channel Copper-Tin-Sulphur Thin-Film Transistor

Narendra Naik Mude, Ravindra Naik Bukke, and Jin Jang\*

Advanced Display Research Center, Department of Information Display,  
Kyung Hee University, Hoegi-dong, Dongdaemun-gu, Seoul 130-701, South  
Korea

Corresponding Author: Jin Jang

\*Email: jjang@khu.ac.kr †

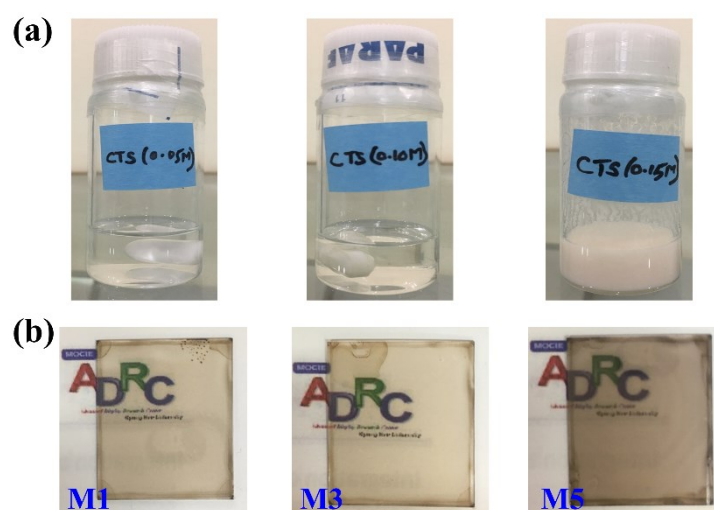


**Figure S1.** The optical photograph of (a) CTS precursor solutions and (b) thin-films using a different precursor solution concentration.

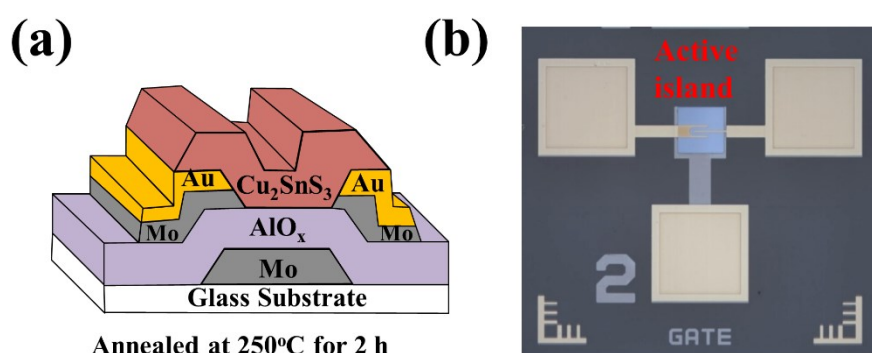


**Figure S2.** Schematic and optical properties of CTS TFT. (a) The schematic cross-sectional view of a bottom-gate, bottom-contact (BGBC) CTS TFT. (b) Optical photograph of the fabricated CTS TFT, with channel width and length of 100 and 10  $\mu\text{m}$ , respectively. A clear active island can be seen.

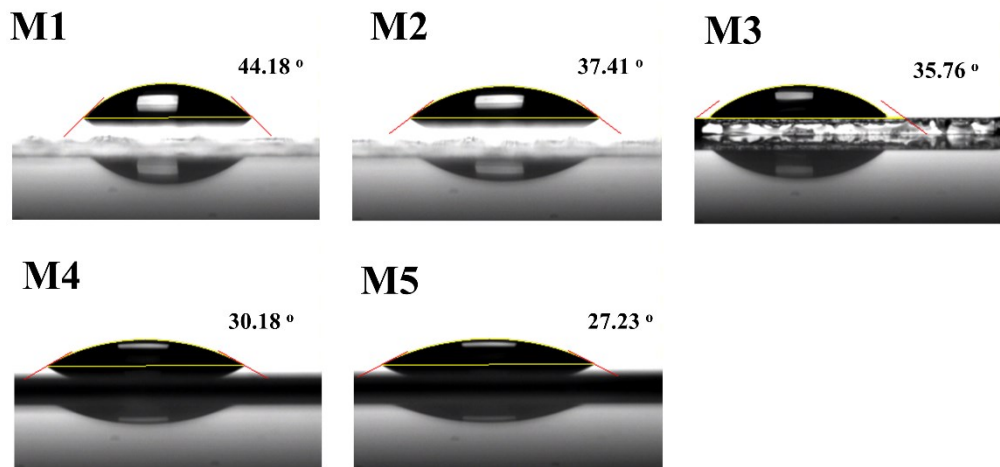


**Figure S3.** Water contact angles of the CTS films with different concentration (M1 = 0.05 M, M2 = 0.075 M, M3 = 0.10 M, M4 = 0.125 M, and M5 = 0.15 M).

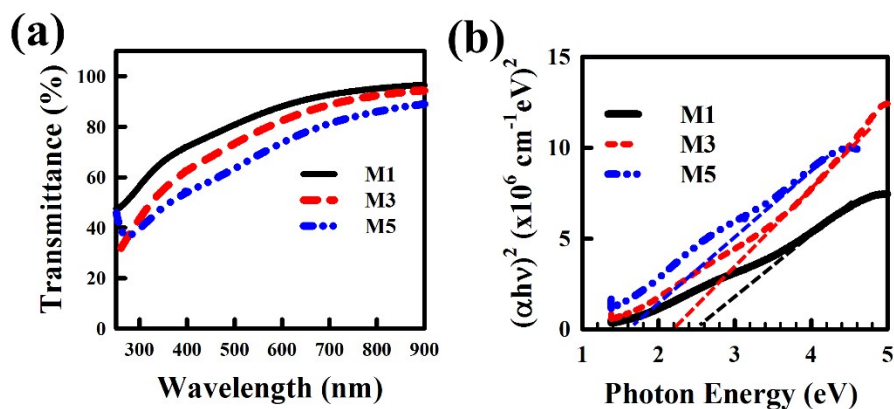


**Figure S4.** Optical properties of CTS thin films. (c) Transmittance and (d) optical bandgap. The bandgaps of CTS thin-films (M1, M3 and M5) are 2.65, 2.30, and 1.85 eV, respectively.

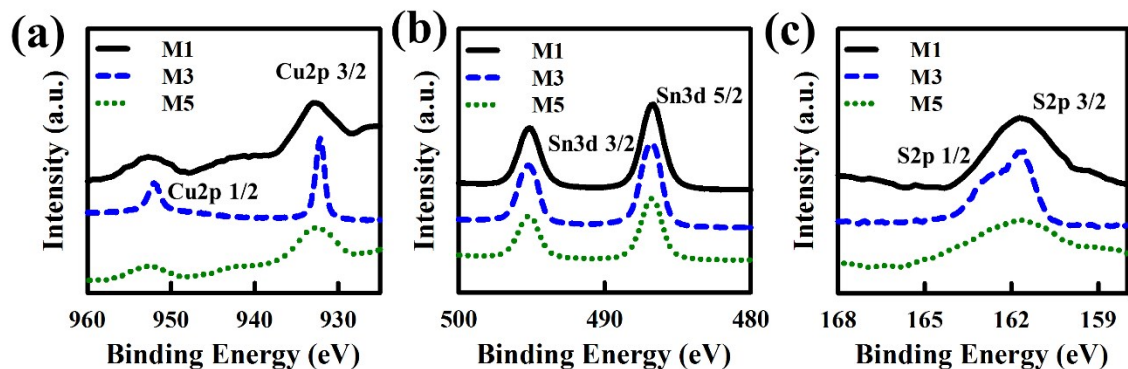


**Figure S5.** The XPS binding energy peaks for the (a) Cu2p, (b) Sn3d, and (c) S2p of CTS (M1, M3, and M5) films.

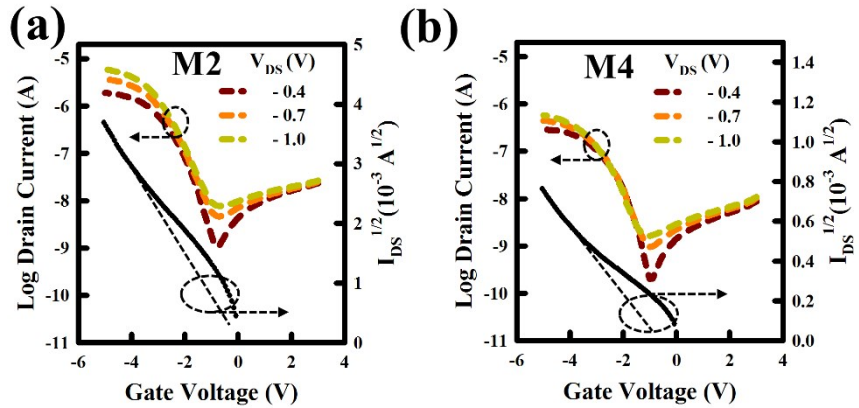


**Figure S6.** The electrical properties of p-type CTS TFTs. The transfer curves of CTS TFTs with different precursor solution concentrations of (a)  $M_2=0.075$  M and (b)  $M_4=0.125$  M. The  $I_{DS}^{1/2}$  vs.  $V_{GS}$ , curves of CTS TFTs, respectively. The mobility was obtained from the linear part of the  $(I_{DS})^{1/2}$  vs.  $V_{GS}$  curve. The transfer curves of the CTS TFTs were measured at drain voltage ( $V_{DS}$ ) = -(0.4, 0.7, and 1) V, by sweeping gate voltage ( $V_{GS}$ ) from +2 to -5 V. All the TFTs have the channel length (L) and width (W) of 10 and 100  $\mu\text{m}$ , respectively.

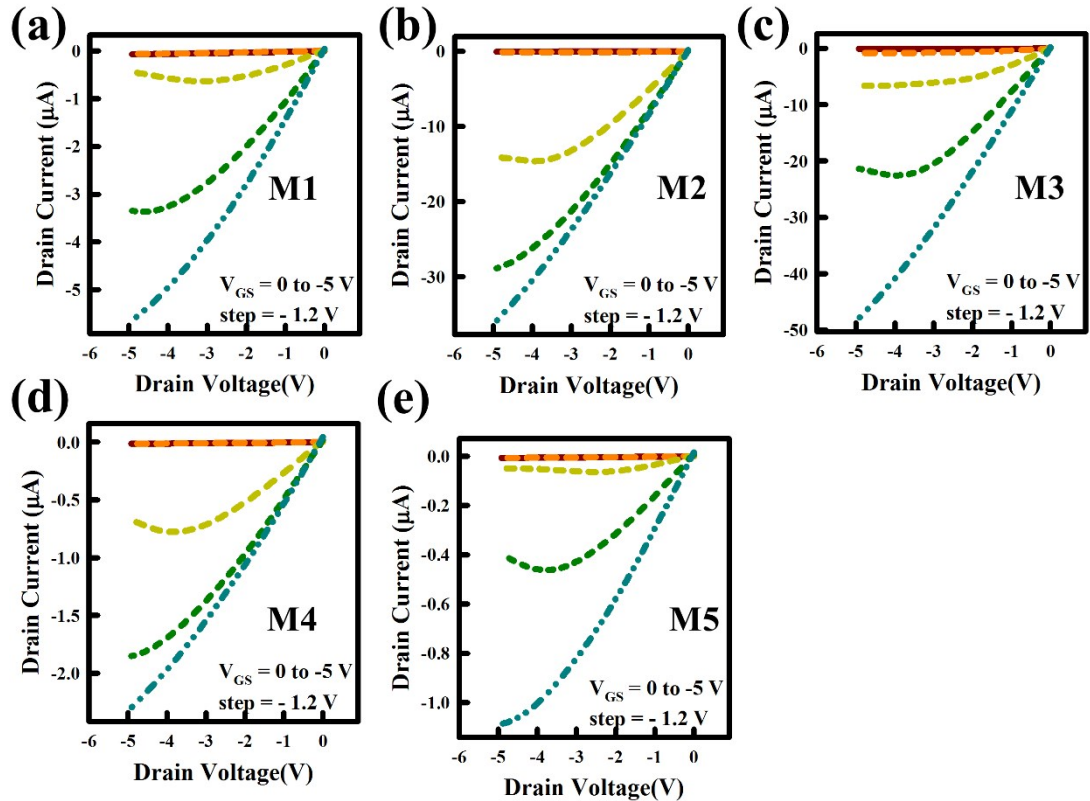


**Figure S7.** The output characteristics of the p-type CTS TFTs with different precursor solution concentrations. Output curves of all the CTS TFTs measured by applying  $V_{GS}$  from 0 to -5 V with a step of -1.2 V. All the TFTs have the channel length (L) and width (W) of 10 and 100  $\mu\text{m}$ , respectively.

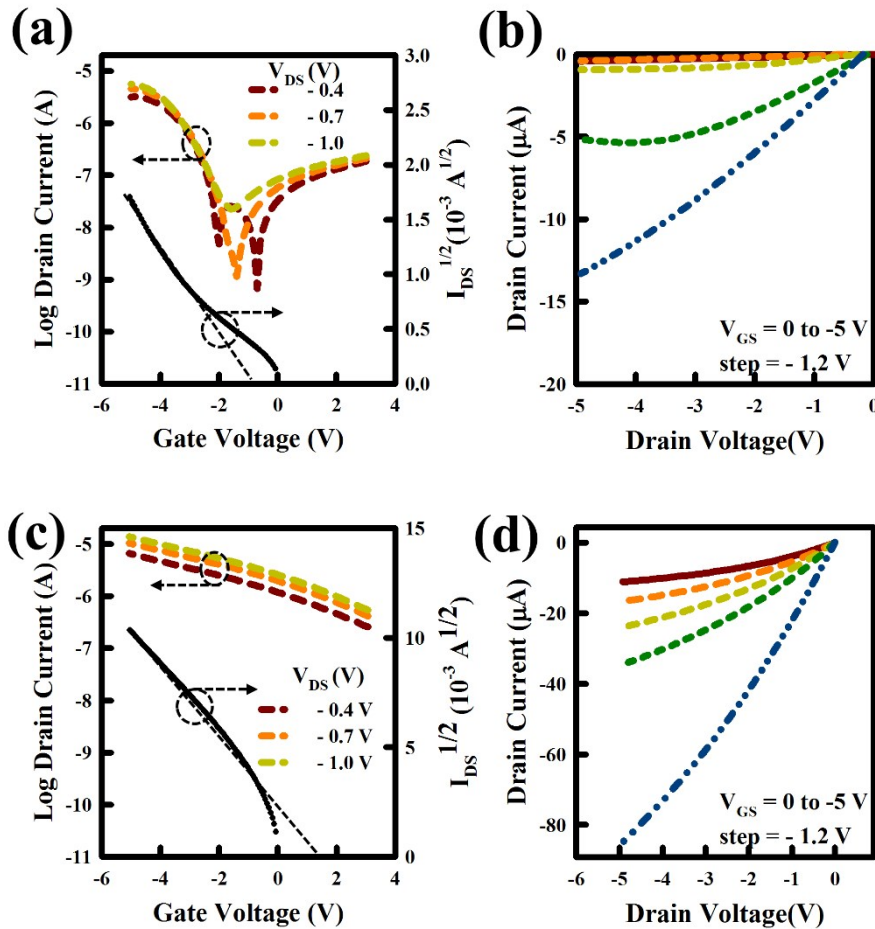


**Figure S8.** The electrical properties of the p-type CTS TFT annealed at 200 and 300°C. (a) The transfer curve and  $I_{DS}^{1/2}$  vs.  $V_{GS}$  curves of CTS TFT. (b) Output curves of the CTS TFT measured by applying  $V_{GS}$  from 0 to -5 V with a step of -1.2 V. (c) Transfer curve and  $I_{DS}^{1/2}$  vs.  $V_{GS}$  curves and (d) output curves of the CTS TFT annealed at 300°C. The transfer curves of CTS TFTs were measured at drain voltage ( $V_{DS}$ ) = -(0.4, 0.7, and 1.0) V, by sweeping gate voltage ( $V_{GS}$ ) from +3 to -5 V.

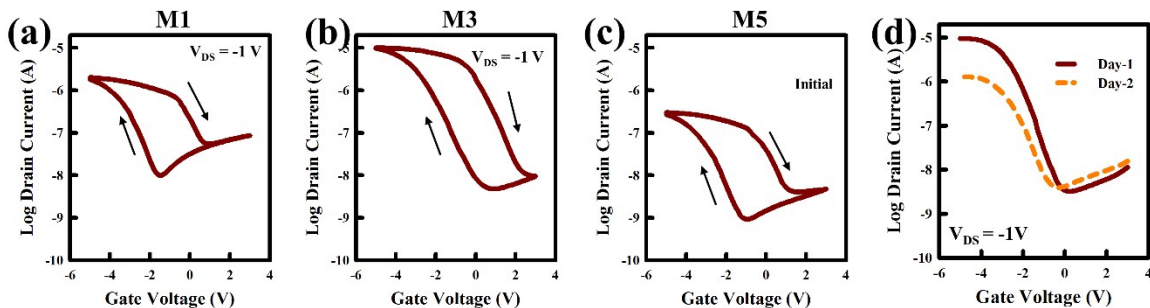
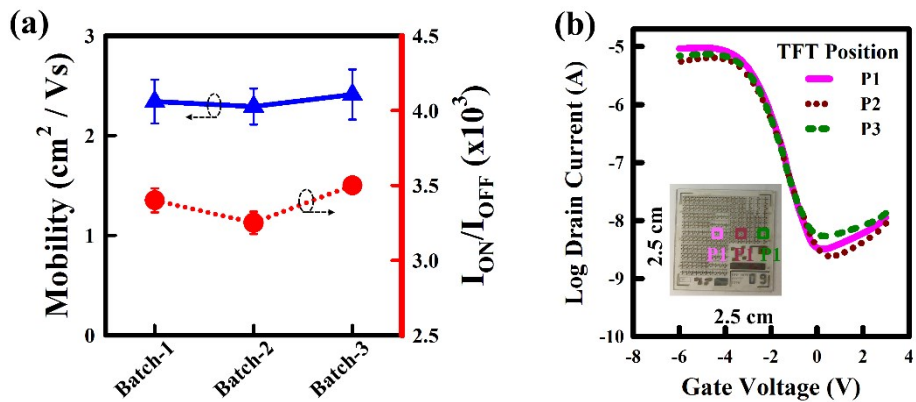


Fig. S9. Transfer curves with hysteresis characteristics for (a) M1, (b) M3 and (c) M5 CTS TFTs. (d) The comparison of transfer curves of CTS TFT measured at Day-1, Day-2, and Day-3, where the TFT were aged in air.



**Fig. S10** (a) Mobility  $I_{\text{ON}}/I_{\text{OFF}}$  of CTS TFT as a function of batches (Batch-1, Batch-2, and Batch-3). (b) Evaluation for the transfer curves of CTS TFT as a function of TFT position. Inset of (b) shows fabricated sample indicating different positions.

**Table S1.** The summary of the water contact angle data for the p-type CTS thin films with different precursor solution concentrations.

Molar Concentration (M)	C.A (deg.)	$\gamma_w$ (mJ/m <sup>2</sup> )	$\gamma_s$ (mJ/m <sup>2</sup> )	W (mJ/m <sup>2</sup> )
0.050	44.18	52.21	38.36	125.01
0.075	37.41	57.83	46.32	130.63
0.100	35.76	59.08	48.44	131.88
0.125	30.18	62.93	54.54	135.73
0.150	27.23	64.74	57.11	137.54

**Table S2.** Hall effect measurement data of p-type CTS thin films with different precursor solution concentrations.

Molar Concentration (M)	Resistivity ( $\Omega/\text{cm}$ )	Mobility ( $\text{cm}^2/\text{Vs}$ )	Conductivity ( $10^{-2}\text{S}/\text{cm}$ )
0.050	0.85	4.02	0.77
0.075	0.75	5.05	1.22
0.100	0.61	9.81	4.30
0.125	0.55	5.10	3.02
0.150	0.41	3.57	2.21

**Table S3.** The summary of the electrical properties of p-type CTS TFTs with different precursor solution concentrations.

<b>Concentration (M)</b>	$\mu_{FE}$ ( $\text{cm}^2 \text{V}^{-1} \text{s}^{-1}$ )	$V_{TH}$ (V)	SS (mV dec $^{-1}$ )	$N_{it}$ ( $10^{12} \text{ cm}^{-2}$ )
0.050	0.24	-1.65	903	7.09
0.075	1.68	-1.25	855	6.69
0.100	2.43	-0.53	664	5.05
0.125	0.11	-0.71	911	7.16
0.150	0.07	-0.82	921	7.24

**Table S4.** The summary of the device performances of the p-type TFTs reported.

<b>Method</b>	<b>Channel</b>	<b>Annealing temp. °C</b>	$\mu_{FE}$ ( $\text{cm}^2 \text{V}^{-1} \text{s}^{-1}$ )	$I_{on}/I_{off}$	<b>Year<sup>ref</sup></b>
Spin coating	SnO	450	0.13	85	2012 <sup>1</sup>
Spin coating	Cu <sub>2</sub> O	700	0.16	$\sim 10^2$	2013 <sup>2</sup>
Spray coating	Cu <sub>2</sub> O	275	$10^{-4}\text{--}10^{-3}$	$1\times 10^{-2}$	2013 <sup>3</sup>
Spin coating	CuSCN	80	$10^{-3}\text{--}10^{-2}$	$\sim 10^4$	2013 <sup>4</sup>
Spin coating	NiO	500	0.14	--	2014 <sup>5</sup>
Spin coating	Cu <sub>2</sub> O	600	0.29	$\sim 10^4$	2015 <sup>6</sup>
Spin coating	CuO	500	0.01	$\sim 10^3$	2016 <sup>7</sup>
Spin coating	NiO	250	0.07	$\sim 10^4$	2016 <sup>8</sup>
Ink-jet printing	CuI	60	4.4	$10^{-1}\text{--}10^{-2}$	2016 <sup>9</sup>
Spin coating	CuO	250	0.32	$\sim 10^4$	2017 <sup>10</sup>
Spin coating	NiO	350	0.01	2	2017 <sup>11</sup>
Spin coating	CuO	500	$2.83\times 10^{-3}$	$\sim 10^4$	2018 <sup>12</sup>
Ink-jet printing	NiO	280	0.78	$5.3\times 10^4$	2018 <sup>13</sup>
Spin coating	CuI	RT	0.44	$10^2$	2018 <sup>14</sup>

## REFERENCES

- (1) K. Okamura, B. Nasr, R. A. Brand, H. Hahn, *J. Mater. Chem.*, 2012, **22**, 4607.
- (2) S. Y. Kim, C. H. Ahn, J. H. Lee, Y. H. Kwon, S. Hwang, J. Y. Lee and H. K. Cho, *ACS Appl. Mater. Interfaces*, 2013, **5**, 2417.
- (3) P. Pattanasattayavong, S. Thomas, G. Adamopoulos, M. A. McLachlan, T. D. Anthopoulos, *Appl. Phys. Lett.*, 2013, **102**, 163505.
- (4) P. Pattanasattayavong, N. Y. Gross, K. Zhao, G. O.N. Ndjawa, J. Li , F. Yan, B. C. O'Regan, A. Amassian and T. D. Anthopoulos, *Adv. Mater.*, 2013, **25**, 1504.
- (5) S. Liu, R. Liu, Y. Chen, S. Ho, J. H. Kim and F. So, *Chem. Mater.*, 2014, **26**, 4528.
- (6) J. Yu, G. Liu, A. Liu, Y. Meng, B. Shin and F. Shan, *J. Mater. Chem., C*, 2015, **3**, 9509.
- (7) J. Jang, S. Chung, H. Kang, V. Subramanian, *Thin Solid Films*, 2016, **600**, 157.
- (8) A. Liu, G. Liu, H. Zhu, B. Shin, E. Fortunato, R. Martins and F. Shan, *Appl. Phys. Lett.*, 2016, **108**, 233506.
- (9) C. H. Choi, J. Y. Gorecki, Z. Fang, M. Allen, S. Li, L. Yu Lin, C. C. Cheng and C. H. Chang *J. Mater. Chem. C*, 2016, **4**, 10309.
- (10) A. Liu, S. Nie, G. Liu, H. Zhu, C. Zhu, B. Shin, E. Fortunato, R. Martins and F. Shan, *J. Mater. Chem. C*, 2017, **5**, 2524.
- (11) Y. Li, C. Liu, G. Wang and Y. Pei, *Semicond. Sci. Technol.*, 2017, **32**, 085004.
- (12) T. S. Jung, H. Lee, S. P. Park, H. J. Kim, J. H. Lee, D. Kim and H. J. Kim, *ACS Appl. Mater. Interfaces*, 2018, **10**, 32337.
- (13) H. Hu, J. Zhu, M. Chen, T. Guo, F. Li, *Appl. Phys. Lett.*, 2018, **441**, 295.
- (14) A. Liu, H. Zhu, W. T. Park, S. J. Kang, Y. Xu, M. G. Kim and Y. Y. Noh, *Adv. Mater.*, 2018, **30**, 1802379.